11th International Conference
on Clouds and Precipitation, 1992.

ANALYSIS OF A TORNADIC SUPERCELL USING AIRBORNE DOPPLER RADAR

David O. Blanchard*
NOAA/NSSL/Mesoscale Research Division
Boulder, Colorado

1. BACKGROUND

During the spring of 1991, the National Severe Storms Laboratory conducted the COPS-91 (Cooperative Oklahoma Profiler Studies-1991) field program in Oklahoma and the Texas Panhandle. Among its goals were (1) an assessment of the recently deployed National Weather Service (NWS) profiler demonstration network in observational studies of mesoscale convective systems (MCSs), (2) documentation of electrification mechanisms in MCSs, and (3) a detailed study of the dryline.

On the afternoon of 26 May 1991, a thunderstorm developed along the dryline on the Texas Panhandle–Oklahoma border and began to move to the east. Within a short time, the storm had reached severe proportions and large hail and tornadoes were reported. The NOAA P-3 aircraft made multiple passes on the west and south sides of the supercell thunderstorm during and after tornado touchdown, gathering extensive pseudo-dual Doppler radar data. The thunderstorm passed close to the Vici, Oklahoma, network profiler, which was recording vertical wind profiles every 5 minutes.

This paper examines the P-3 Doppler-derived horizontal winds and compares them with the winds from the profiler at Vici. Also, some of the fine-scale circulations and storm structure observed by the P-3 are discussed in the context of current modeling results and understanding of tornadic supercells. Finally, changes in the pre-storm environmental winds are examined.

2. P-3 DATA

The X-band vertically pointing Doppler radar system on the P-3 was recently upgraded to employ the fore-aft scan technique, or FAST (Jorgensen and DuGranrut 1991). This procedure consists of alternatively scanning the P-3's tail radar antenna forward, then aft, about 25° of normal to the aircraft heading. The P-3 has only a single radar and antenna, so the antenna must be mechanically slewed to point in the desired direction. Along a radial, data are collected in bins of 75, 150, and 300 m, depending on the range from the aircraft. The antenna rotation rate (~10 rpm) produces an effective horizontal data spacing of ~1 km at typical P-3 ground speeds (~120 m s^{-1}). FAST allows the P-3 to collect pseudo-dual Doppler radar while following a straight flight track

The data were processed with a series of programs to edit and transform the slewed radial data into *u*- and *v*-wind components. The first step in the editing takes place in radar space. Ground clutter and "2nd trip" contamination is deleted and the aircraft motion is removed from the radial velocity data. Next, the data are examined for aliased velocities and "unfolded." Because the Nyquist interval for this radar is ±12.9 m s^{-1} and the ambient shear for this case is large (> 50 m s^{-1} through the depth of the troposphere), there were multiple folds. This process is repeated for each scan. The next step is to convert the radial data to a Cartesian grid and edit the data in regions that may have been unfolded incorrectly in the first step.

3. PROFILER DATA

The profiler data are from Vici, Oklahoma, which is one of the many NWS profiler demonstration sites currently in operation in the central region of the United States. Data are collected from three beams: one points vertically, and the other two are pointed 15° from the vertical and are oriented toward the north and east. Conversion of Doppler radial velocities along the north and east beams to *u*- and *v*-components of the horizontal wind uses the geometry of the beam angles and accounts for the vertical motion using the vertically pointing beam. Besides radial velocity, returned power and spectral variance were also measured and recorded. This information is useful in determining the validity of the derived *u*- and *v*-components of the horizontal wind.

4. AIRCRAFT DOPPLER RESULTS

Figure 1 is the result of the pseudo-dual Doppler synthesis of horizontal winds. The winds are storm relative: storm motion was 270° at 8 m s^{-1}.

It is obvious that a cyclonic circulation is present at x = 29, y = 17. Wind speeds to the south and southwest of the circulation are ~30 m s^{-1} and greater. The mesocyclone is strongest at this level and weakens aloft, although cyclonic vorticity is present through a deep layer. Reflectivities show a typical "hook echo" in the same region as the mesocyclone. Figure 2 shows

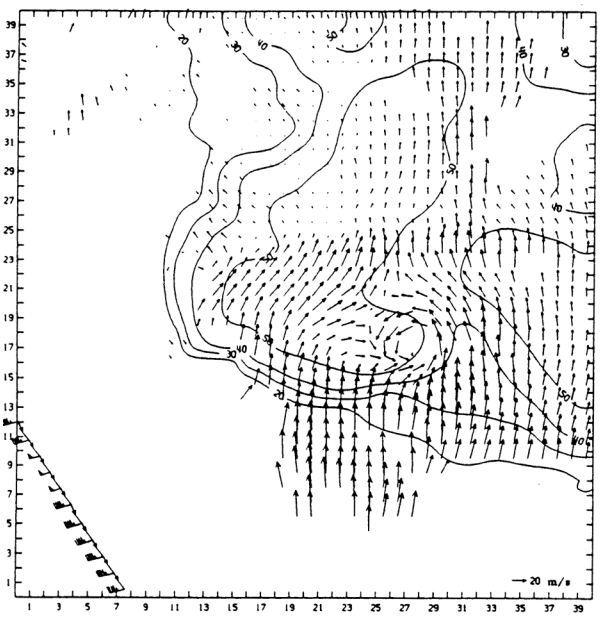

Figure 1. Storm reflectivity and synthesized dual-Doppler winds from the NOAA P-3 aircraft tail radar. Grid is 40 km on a side. Altitude is 1.5 km above ground level (AGL). Aircraft flight track and flight-level (~4.4 km) winds are plotted in the lower left corner. Winds are storm relative using a storm motion of 270° at 8 m s^{-1}. Scale for wind vectors is given in the lower right corner. Radar reflectivity contours are every 10 dBZ, starting at 20 dBZ.

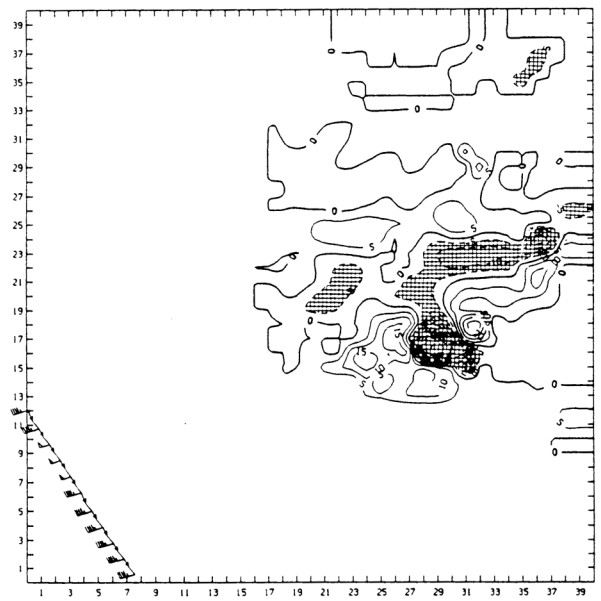

Figure 2. As in Fig. 1, except for vertical velocity and altitude of 2.5 km AGL. Contours every 5 m s^{-1}. Solid (dashed) contours are updrafts (downdrafts). Zero contour is double width. Downdrafts are hatched.

the vertical velocities at this level. These velocities were computed through upward integration of the continuity equation and were mass balanced using the O'Brien (1970) technique and assuming that $w = 0$ at the surface. Note the strong downdraft of -40 m s^{-1} adjacent to an updraft of +30 m s^{-1}. The mesocyclone shown in Fig. 1 straddles these two draft structures. Observational and modeling work by Lemon and Doswell (1979), Klemp et al. (1981), and Wicker and Wilhelmson (1992) suggests that tornadogenesis requires the presence of an updraft/downdraft couplet similar to that shown here.

There are uncertainties associated with the strength of these vertical drafts. This is due to two problems with the airborne Doppler data. Owing to ground clutter contamination, winds at the lowest level (0.5 km) were suspect, so low-level divergence is near zero close to the ground. The second problem existed at the upper levels. The radar velocity data were very noisy at the top of the updraft, and good divergence values there are also suspect. Clearly the loss of this information affects the computation of draft strength. The velocities shown here can be considered lower limits, and the actual drafts were probably much stronger.

It is useful to speculate on the cause of the noisy data at high levels. Because the wind structure in the lowest kilometer or two of the atmosphere is strongly sheared in both direction and speed, the relative helicity (Davies-Jones 1984; Davies-Jones and Burgess 1990) is high. Lilly (1986) has shown that high helicity reduces turbulence in the updraft. At the top of the updraft, relative helicity is weaker because there is little shear at this level. As the updraft passes the equilibrium level, it rapidly decelerates and, without the stabilizing effect of helicity, turbulent flow increases. Because the radar averages pulses over many turbulent eddies, the spectral width of the estimate increases, resulting in a noisy mean estimate of the wind. This problem was not noted to such a large degree with other storms on this day. This suggests that the radar was probably working properly and that this thunderstorm was extreme in its draft structure.

5. PROFILER RESULTS

Figure 3 shows the 5-min horizontal winds from the surface to 17 km (AGL) from 2200 to 2348 UTC on 26 May 1991. (The profiler experienced problems after this time, and only l-h data are available.) The most obvious feature is the almost unchanging winds through a large portion of the troposphere. The most significant changes occurred in the lowest 1 km where the winds strengthened and backed slightly, and near the

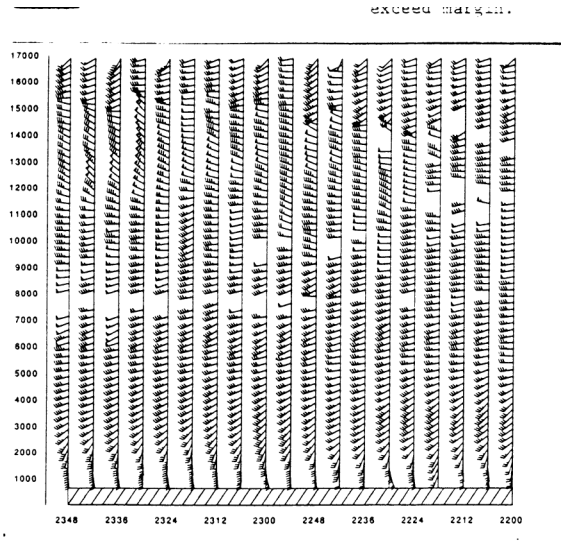

Figure 3. Vertical profile of horizontal winds obtained from the NOAA wind profiler at Vici, Oklahoma. Time increases from right to left. Wind profiles are every 6 minutes. Height scale on the left is in meters AGL. Wind barbs conventional; each barb equal to 5 m s^{-1}, half barbs 2.5 m s^{-1}, and pennants 25 m s^{-1}.

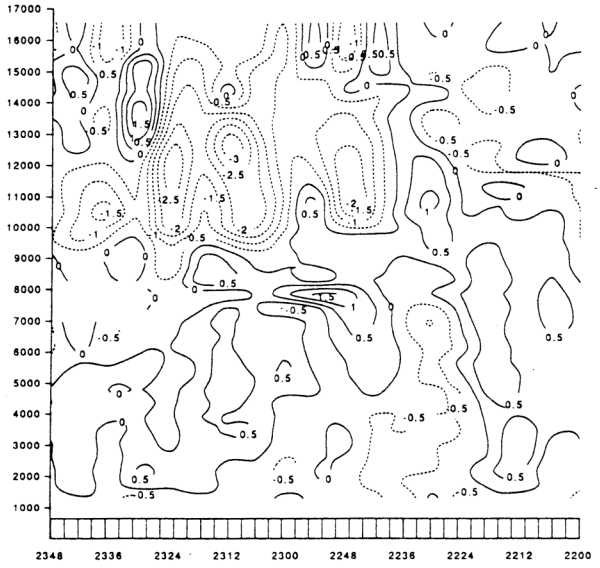

Figure 4. As in Fig. 3, except for vertical velocity. Contours every 0.5 m s^{-1}; solid contours positive.

tropopause where the winds acquired a more northerly component. The probable cause of the changes at the upper levels is the approaching thunderstorm. A time plot of returned power (not shown) indicates that the anvil passed overhead in the 10–15 km layer starting at 2230 UTC. Downward vertical velocities associated with this feature (Fig. 4) are 2–3 m s^{-1}. Because the 404 MHz profiler is sensitive to hydrometeors, it is possible that these velocities are the result of ice crystals and hail falling from the anvil. The increasing northerly component could be an artifact of hydrometeors affecting the vertical component of the wind used to correct the horizontal winds. It could also be a basic sampling problem related to inhomogeneities in the anvil between where the north beam is pointing and the vertical beam. For example, at 16-km altitude, the vertical beam and the north beam are 4 km apart and they may be sampling very different vertical velocities. On the other hand, winds from the P-3 Doppler analysis at this altitude show northwest winds on the south side of the anvil, lending credibility to the profiler results.

An interesting updraft in the profiler data originate near the surface at 2212 UTC, and reaches a height of 12 km at 2230 UTC and 16 km at 2242 UTC. A downdraft appears next to the updraft and exhibits the same magnitude and tilt as the updraft. This may be an example of a (gravity) wave passing over the profiler, but it does not appear to be related to the subsequent development of convection.

Another feature of interest is the returned power in the lowest few kilometers (not shown). The region of strongest return indicates the turbulence of the convective boundary layer. The depth of this layer increases during the afternoon, and at about 2212 UTC a convective plume breaks through into the middle troposphere. Satellite images at this time indicate that (moist) convective activity had just developed to the west of the profiler. These data may be useful in forecasting when shallow convection will break through the top of the boundary layer.

6. SUMMARY

A brief analysis has been presented of a tornadic supercell and its environment. The supercell was documented with airborne Doppler radar using FAST while the environment was being sampled every 5 minutes by a vertically-pointing Doppler-wind profiler within the NWS profiler demonstration network. Synthesis of horizontal winds from the airborne radar showed a well-defined mesocyclone at the lowest levels and cyclonic vorticity aloft. The mesocyclone and the tornado were in a region of strong gradient between an updraft and a downdraft. The strong downdraft is connected to a larger, but weaker region of downdraft to the north and east of the mesocyclone. Because no Doppler data before this time were available, the evolution of these features cannot be documented. Observational and modeling studies suggest that the presence of this downdrafts is critical for tornado-genesis. It must be pointed out that the tornado was dissipating when the aircraft arrived. The structure

revealed by the radar is that of a post-tornadic storm and differs from most tornadogenesis models and observations that focus on the pre-tornadic environment.

The profiler at Vici, Oklahoma, was ~35 km south of the mesocyclone. At this distance, the only significant environmental changes are a strengthening and slight backing of the wind in the lowest levels and strongly veered winds near the tropopause. These veered winds may be an artifact resulting from falling hydrometeors, or they may be related to the strongly divergent flow in the thunderstorm anvil. The lack of a strong signal in the low-level environmental winds suggests, in this case at least, that the effects from the storm are not strong at this distance. Possibly other techniques, such as computing the perturbation wind from a moving time average, might provide more information to a forecaster.

Even though the profiler did not note large environmental changes as the storm passed, it is useful for assessing the potential for severe storm development in a sheared, convectively unstable environment. The environmental winds before the tornado show the classic veered profile associated with supercell thunderstorms. This information was used successfully by severe storm forecasters during the warm season.

Acknowledgements. Thanks are extended to J. Augustine (NOAA/NSSL) for allowing me to borrow his code to retrieve the vertical velocities from the profiler data. Special thanks to D. Van de Kamp (NOAA/FSL) for his efforts to recover the missing profiler data necessary for this case study. The airborne Doppler analysis code is the result of work by B. Smull and D. Jorgensen(NOAA/NSSL)

REFERENCES

Davies-Jones, R, 1984: Streamwise helicity: The origin of updraft rotation in supercell storms. *J. Atmos. Sci.*, **41**, 2991–3006.

_____, and D. Burgess, 1990: Test of helicity as a tornado forecast parameter. *Preprints, 16th Conf. Severe Local Storms*, Kannanaskis, AB, Amer. Meteor. Soc., 588–592.

Jorgensen, D. P ., and J. D. DuGranrut, 1991: A dual-beam technique for deriving wind fields from airborne Doppler radar. *Preprints, 25th Intl. Conf. on Radar Meteor.*, Paris, Amer. Meteor. Soc., 458-461.

Klemp, J. B., R. B. Wilhelmson, and P. S. Ray, 1981: Observed and numerically simulated structure of a mature supercell thunderstorm. *J. Atmos. Sci.*, **38**, 1558–1580.

Lemon, L. R., and C. A. Doswell III, 1979: Severe thunderstorm evolution and mesocyclone structure as related to tornadogenesis. *Mon. Wea. Rev.*, **107**, 1184–1197.

Lilly, D. K., 1986: The structure, energetics and propagation of rotating convective storms. Part II: Helicity and storm stabilization. *J. Atmos. Sci.*, **43**, 126–140.

Wicker, L. J. and R. B. Wilhelmson, 1992: Numerical simulation of tornadogenesis within a supercell thunderstorm. *Proceedings, Tornado Symposium III* (C. Church, Ed.), Amer. Geophy. Union (in press).

11th International Conference
on Clouds and Precipitation, 1992.